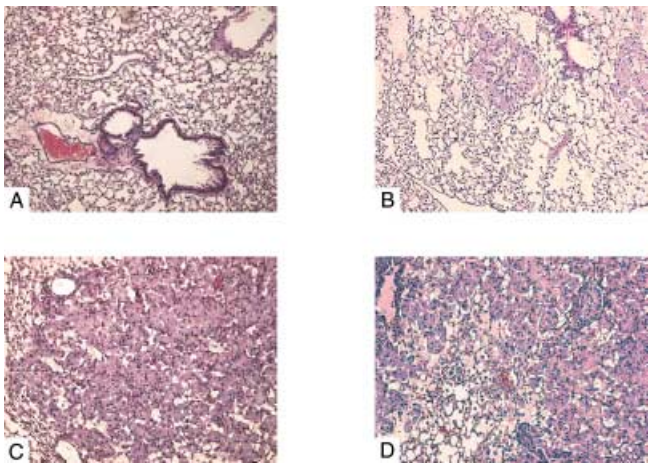

Figure 5. Histological characteristics of the lung tumors: The tumor tissue shows prominently roundly formed nuclei and a solid structure; operatively expansive. A) and B) Haematoxylin and Eosin staining of lung tissue of a treated mouse; the tumor tissue is only located in small areas. C) and D) Haematoxylin and Eosin staining of lung tissue of a control mouse; tumor invading the bronchius.

solubility arising from its hydrophilic sugar moiety and the fact that it seems not to penetrate the cell membrane. Thus, cellular human galactosidase may be used for an activation. Finally, the synthesis allows the preparation of analogues containing different sugar moieties.

Received: September 27, 2001 [Z17982]

[1] Reviews: a) L. N. Jungheim, T. A. Shepherd, *Chem. Rev.* **1994**, *94*, 1553 – 1566; b) C. J. Springer, I. Niculescu-Duvaz, *Adv. Drug Delivery Rev.* **1997**, *26*, 151 – 172; c) K. N. Syrigos, A. A. Epenetos, *Anticancer Res.* **1999**, *19*, 605 – 614; G. M. Dubowchik, M. A. Walker, *Pharmacol. Ther.* **1999**, *83*, 67 – 123.

[2] K. D. Bagshawe, *Br. J. Cancer* **1987**, *56*, 531 – 532.

[3] Our early investigations using acetal glycosides of aldophosphamide as prodrugs were not successful probably because of the relatively low cytotoxicity of aldophosphamide: a) L. F. Tietze in (Eds.: E. Borowski, D. Shugar), *Molecular aspects of chemotherapy*, Pergamon Press, Oxford, **1990**, p. 55; b) L. F. Tietze, R. Fischer, *Angew. Chem.* **1981**, *93*, 1002; *Angew. Chem. Int. Ed. Engl.* **1981**, *20*, 969; c) L. F. Tietze, R. Fischer, H. J. Guder, A. Goerlach, M. Neumann, T. Krach, *Carbohydr. Res.* **1987**, *164*, 177 – 194; d) L. F. Tietze, M. Beller, R. Fischer, M. Lögers, E. Jähde, K. H. Glüsenkamp, M. F. Rajewsky, *Angew. Chem.* **1990**, *102*, 812 – 813; *Angew. Chem. Int. Ed. Engl.* **1990**, *29*, 782 – 783.

[4] L. F. Tietze, T. Herzig, A. Fecher, F. Haunert, I. Schuberth, *ChemBioChem* **2001**, *2*, 758 – 765.

[5] Reviews: a) D. L. Boger, D. S. Johnson, *Angew. Chem.* **1996**, *108*, 1542 – 1580; *Angew. Chem. Int. Ed. Engl.* **1996**, *35*, 1438 – 1474; b) D. L. Boger, R. M. Garbaccio, *Acc. Chem. Res.* **1999**, *32*, 1043 – 1052.

[6] M. Ichimura, T. Ogawa, K. Takahashi, E. Kobayashi, I. Kawamoto, T. Yasuzawa, I. Takahashi, H. Nakano, *J. Antibiot.* **1990**, *43*, 1037 – 1038.

[7] a) L. F. Tietze, R. Hannemann, W. Buhr, M. Lögers, P. Menningen, M. Lieb, D. Starck, T. Grote, A. Döring, I. Schuberth, *Angew. Chem.* **1996**, *108*, 2840 – 2842; *Angew. Chem. Int. Ed. Engl.* **1996**, *35*, 2674 – 2677; b) L. F. Tietze, M. Lieb, T. Herzig, F. Haunert, I. Schuberth, *Bioorg. Med. Chem.* **2001**, *9*, 1929 – 1939.

[8] D. L. Boger, S. W. Boyce, R. M. Garbaccio, M. Searcey, Q. Jin, *Synthesis* **1999**, 1505 – 1509.

[9] We have also prepared a methyl-CBI-galactoside with a secondary chloride moiety, which also shows a higher selectivity than **2** but with a significantly reduced cytotoxicity of the corresponding drug, see ref. [4].

[10] a) R. R. Schmidt, *Angew. Chem.* **1986**, *98*, 213 – 236; *Angew. Chem. Int. Ed. Engl.* **1986**, *25*, 212 – 235; b) W. Dullenkopf, J. C. Castro-Palomino, L. Manzoni, R. R. Schmidt, *Carbohydr. Res.* **1996**, *296*, 135 – 147.

[11] a) M. A. Warpehoski, *Tetrahedron Lett.* **1986**, *27*, 4103 – 4106; b) S. Rajeswari, A. A. Adesomoju, M. P. Cava, *J. Heterocycl. Chem.* **1989**, *20*, 557 – 564; c) D. L. Boger, W. Yun, N. Han, *Bioorg. Med. Chem.* **1995**, *3*, 1429.

[12] R. Appel, *Angew. Chem.* **1975**, *87*, 863 – 874; *Angew. Chem. Int. Ed. Engl.* **1975**, *15*, 801 – 812.

[13] Severe combined immunodeficient (SCID) mice, strain C.B-17/Ztm-scid, 10 – 12 weeks old, were used.

[14] F. Alves, U. Borchers, B. Pladge, H. Augustin, K. Nebendahl, G. Klöppel, L. F. Tietze, *Cancer Lett.* **2001**, *165*, 161 – 170.

[15] M. P. Napier, S. K. Sharma, C. J. Springer, K. D. Bagshawe, A. J. Green, J. Martin, S. M. Stribbling, N. Cushen, D. O'Malley, R. H. J. Begent, *Clin. Cancer Res.* **2000**, *6*, 765 – 772.

Magnetization of Chiral Monolayers of Polypeptide: A Possible Source of Magnetism in Some Biological Membranes**

Itai Carmeli, Viera Skakalova, Ron Naaman,* and Zeev Vager

Some biological membranes are affected by weak magnetic fields.[1] In particular, magnet-induced orientation was observed in the outer segments of retinal rods,[2] chloroplasts,[3] bacterial chromatophores,[4] purple membranes,[5] and recently in black lipid membranes.[6] The membrane surfaces tend to align perpendicular to the magnetic field. Alignment due to anisotropic magnetic susceptibility,[7] which explains alignment effects in liquid crystals, requires much higher magnetic fields than were used in the above experiments. Hence, no existing theory could explain these significant observations. The lack of physico-microscopic understanding of the effect of magnetic fields on biological membranes prevents the comprehension of its significance.

By studying well-characterized monolayers of polyalanine we were able not only to obtain results similar to those observed in biological membranes, but also to gain an insight into the details of a mechanism that may account for the previously observed magnetic behavior of membranes. We propose an explanation of these phenomena in terms of a physical model, the components of which are supported by the experimental results presented here.

Self-assembled monolayers of L- or D-polyalanine polypeptides in the form of α-helices were prepared on glass slides coated with a 100-nm thick annealed gold film. The orientation of the molecules was monitored by IR spectroscopy in the presence and absence of a magnetic field. In addition, we

[*] Prof. R. Naaman, I. Carmeli, Dr. V. Skakalova, Prof. Z. Vager
Department of Chemical Physics
Weizmann Institute of Science
Rehovot 76100 (Israel)
Fax: (+972) 8-9344123
E-mail: ron.naaman@weizmann.ac.il

[**] We are grateful to Prof. M. Fridkin and his group for helping us in the synthesis of the polyalanine. Partial support from the US – Israel Binational Science Foundation is acknowledged.

  1433-7851/02/4105-0761 $ 17.50+.50/0

investigated the selectivity of the layers towards spin-polarized electron transmission.

Connecting a sulfide group at the C- or N-terminus of the peptide makes the dipole moment of the attached molecules point away from or towards the substrate. Three types of films were investigated: poly(L-alanine) and poly(D-alanine), both connected to the surface at the C-terminus (LC and DC, respectively), and poly(D-alanine) connected to the surface at the N-terminus (DN). Polypeptide lengths between 16 and 22 amino acid units were used. The structure of the films was determined by means of their FT-IR spectra.[8] The handedness of the adsorbed films was verified by circular dichroism absorption, and their thickness was measured by ellipsometry. Atomic force microscopy (AFM) was also carried out. All the results reported here were obtained at room temperature from close-packed layers.

The IR spectra of LC and DC monolayers were measured at magnetic field strengths of 0, ± 900, and ± 4500 G applied perpendicular to the layer. Henceforth, "N" indicates magnetic field lines starting at the North Pole and penetrating through the gold surface to the monolayer, and vice versa for "S". Figure 1 shows grazing-angle IR spectra obtained for the

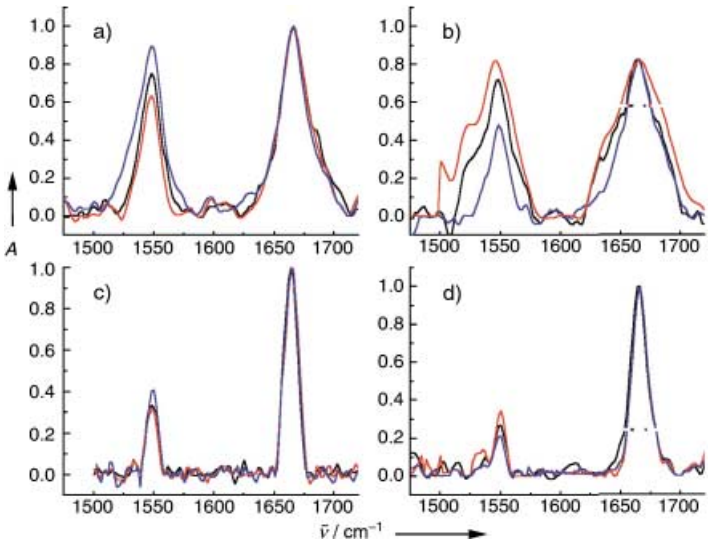

Figure 1. IR spectra of DC (a and c) and LC layers (b and d) showing the amide I (ca. 1665 cm^{-1}) and II bands (ca. 1550 cm^{-1}). The spectra are normalized to the peak of the 1665-cm^{-1} band. The spectra were recorded with S (red) or N magnets (blue) or without a magnetic field (black). The spectra in a and b were recorded at 4500 G, and those in c and d at 900 G. A = absorbance.

vibrations of the amido group.[9] The amide I vibration is parallel to the molecular axis (at ca. 1665 cm^{-1}), while the amide II vibration at about 1550 cm^{-1} is perpendicular to the axis. The spectra are normalized to the peak of the 1665-cm^{-1} band. If the molecules are oriented normal to the surface, the intensity of the amide II component vanishes because the metal substrate cancels the transition dipole moment. Hence, the ratio between the intensity of the two peaks provides a direct measure of the tilt angle of the molecules relative to the surface normal.[10]

From Figure 1 it is evident that the magnetic field affects the relative IR intensities. For the two LC layers (Figure 1b, d) S fields increase the average tilt angles, while N fields decrease them. The reverse is true for the DC layers (Figure 1a, c); that is, S fields decrease the average tilt angles, while N fields increase them. Larger fields lead to larger tilts. It takes 2–6 h for the effect of the magnetic field on the tilt angle to reach equilibrium. The time required depends on the strength of the magnetic field and on the quality of the monolayer, that is, its packing density and the average tilt angle. Denser layers require more time for equilibration in magnetic fields. The above magnetic-orientation effects within the layers provide clear evidence that the films have magnetic properties and that opposite magnetization occurs for opposite handedness. Classic magnetization of iron is interpreted as orientation of domains, and the magnetic orientation of these artificial LC and DC monolayers mimics orientational effects already found in biological membranes.[5]

For the electron transmission studies, the samples were inserted into an ultrahigh vacuum chamber at $< 10^{-8}$ mbar. Polarized photoelectrons were ejected from the substrate by applying a 248-nm laser beam with a $\lambda/4$ plate to create left- or right-handed circularly polarized light. Right-handed circularly polarized light induces positive helicity[11] in the photoelectrons ejected from the gold substrate, and vice versa for left-handed polarized light. The photoelectrons are polarized by about 15%.[12] After passing through the organic layers, energy distribution of the electrons was analyzed by a time-of-flight spectrometer.[13]

Figure 2 presents the kinetic energy distributions of photoelectrons ejected with a left- or right-polarized laser. The spectra in panels a and c were obtained for the transmission of electrons through LC and DC films, and panel b for a DN film. Figures 2a and c confirm earlier results that showed a large asymmetry for the transmission of polarized electrons

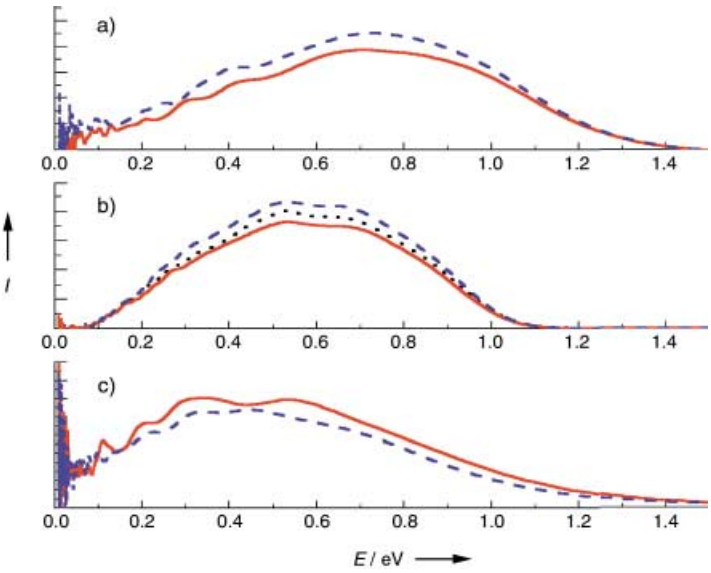

Figure 2. Energy distribution for photoelectrons ejected with a left (negative spin polarization; red, solid) or right circularly polarized laser (positive spin polarization; blue, dashed). The signal obtained with a linearly polarized laser is shown as a dotted black line. The electrons were transmitted through LC (a), DC (b), and DN films (c). I = intensity.

  1433-7851/02/4105-0762 $ 17.50+.50/0

through organized films of chiral molecules.[14] The sign of the asymmetry depends on the handedness of the molecules. Surprisingly, for a given handedness of the molecules the sign of the asymmetry switches upon reversing the way the molecules are adsorbed on the surface (from N- to C-bound molecules). This is clearly seen in Figures 2b and c. The observed asymmetry[15] in the transmission through the layer of photoelectrons produced by left and right circularly polarized photons changes from 0.09 ± 0.02 to -0.10 ± 0.02 (Figures 2b and 2c, respectively). Importantly, the observed effect of 10% is induced by a mere 15% polarization of the photoelectrons.[12] Thus, the selectivity for the incoming helicity of the electrons is as high as 70%, and considering experimental error could be even higher.

Several questions arise from the above observations.

- Why are the layers magnetic?
- Why is there a relation between the direction of magnetism and the handedness of the molecules?
- Why is there a large spin selectivity for electron transmission?
- Why does it change sign with both change of handedness and change in the direction of the molecular electric dipole?

Before introducing a possible model for answering the above questions, a few remarks on some known physics of the observed phenomena are appropriate. In solution polyalanine molecules have a large electric dipole moment of about 50 D.[16, 17] When the molecules are attached as a monolayer, they must lose most of their dipole moment; otherwise the repulsion between them would prevent close packing. Simple electrostatic arguments[18] indicate that the molecular dipole moment must be reduced by more than an order of magnitude. A direct indication of the dipole moment of adsorbed molecules can be obtained from the substrate's work function. From the high-energy cutoff of the photoelectron spectra (Figure 2) it is evident that upon reversing the direction of the layer from C- to N-bound (Figures 2a, c vs b), the work function increases by only about 0.3 eV, whereas for molecules with a dipole moment of about 10 D or more the work function would have dropped by many volts. This means that the dipole moment of the molecules was reduced by two orders of magnitude due to adsorption.[19] Theory indeed predicts that the molecular dielectric constant will be modified substantially by adsorption as a monolayer.[14, 20, 21] This means that the electronic structure of the molecules is substantially modified upon adsorption, probably by charge transfer between the metal substrate and the molecule. Apparently, the charge redistribution process results in unpaired electrons on the adsorbed molecules, that is, the adsorbed molecules become paramagnetic.

Still, the questions posed above are not answered. A full description of these phenomena does not yet exist, but the following simple model is compatible with all the observations and correctly predicts the direction of magnetization. Moreover, since the reported phenomena exhibit parallels to some biological membranes, the model may serve as a basis for understanding the effects of magnetic fields on biological systems.

Upon adsorption, a transient current flows through the helix and discharges the electric dipole while inducing magnetism, like a classical electromagnetic coil. The spins of simultaneously created unpaired electrons adjust accordingly and remain polarized with the support of exchange forces with the metal and the already polarized electrons of attached neighboring helices. The result of such an adsorption mechanism is a magnetic layer in which the direction of the magnetic field is given by Ampere's law. For each adsorbed helix, the original electric dipole polarity and the handedness of the helix determine the direction of the magnetic field along the helical axis.

As can be seen in Figure 1, the helix axes are not well aligned normal to the surface. Therefore, when an external magnetic field is applied in the normal direction, it forces these axes to become closer to or further away from normal, depending on the direction of the external magnetic field. The observed magnetic effects in Figure 1 are consistent with this simple model.

The magnetic properties of the film are the reason for the large spin selectivity in electron transmission. This effect is consistent with the effect in inorganic thin magnetic layers, known as giant magneto spin selectivity[22, 23] and the related colossal magnetoresistance effect.[24, 25] Hence, the magnetic properties of the organic films explain their high selectivity for transmission of spin-polarized electrons, an effect that results from the cooperative nature of the film on the metal substrate. The seemingly surprising change in the direction of magnetization on changing the molecular terminus on the gold surface is resolved by the direction of discharge of the electric dipole through the helices.

In conclusion, we found that the adsorption of chiral species in layers converts electric dipoles into magnetic dipoles. Some biological membranes that show similar magnetic orientation effects can be expected to have similar magnetic properties.

Received: August 28, 2001 [Z17805]

[1] For example, see T. S. Tenforde in *Handbook of Biological Effects of Electromagnetic Fields* (Eds.: C. Polk, E. Postow), CRC, Boca Raton, **1996**, p. 185.
[2] N. Chalazonitis, R. Changeux, A. Arvanitai, *C. R. Acad. Sci. Ser. D* **1970**, *271*, 130–133.
[3] N. E. Geacintov, F. Van Nostrand, M. Pope, J. B. Tinkel, *Biochim. Biophys. Acta* **1972**, *226*, 486–491; N. E. Geacintov, F. Van Nostrand, J. F. Becker, J. B. Tinkel, *Biochim. Biophys. Acta* **1972**, *267*, 65–79.
[4] J. D. Clement-Metral, *FEBS Lett.* **1975**, *50*, 257–260.
[5] D.-C. Neugebauer, A. E. Blaurock, D. L. Worcester, *FEBS Lett.* **1977**, *78*, 31–35.
[6] S. Ozeki, H. Kurashima, M. Miyanaga, C. Nozawa, *Langmuir* **2000**, *16*, 1478–1480.
[7] J. P. Lu, *Phys. Rev. Lett.* **1995**, *74*, 1123–1126.
[8] In helical peptides, the transition moment of the amide I band lies nearly parallel to the helix axis, and that of amide II perpendicular. Transition moments parallel to the gold surface cannot be detected in grazing-angle FT-IR. The ratio between the amide I (1665 cm^{-1}) and II bands (1550 cm^{-1}) indicates the extent to which the molecules in the monolayer are oriented perpendicular to the gold surface.
[9] *Peptides, Polypeptides and Proteins* (Ed.: E. R. Blout), Wiley, New York, **1974**, p. 379.
[10] Since polyalanine is hydrophobic, it is difficult to purify the sample by chromatography and to obtain a single-size polypeptide. Hence, the samples tend to vary in the distribution of peptide length from batch to batch. This is expressed by the spread in tilt angles of the different layers, which was larger for less uniform batches. However, the results

  1433-7851/02/4105-0763 $ 17.50+.50/0

obtained were consistent for all selected samples. Samples were rejected if the average tilt angle exceeded 50°.
[11] The helicity is defined for particles with momentum $\boldsymbol{p}$ and spin $\boldsymbol{s}$ as the expectation value of $\boldsymbol{s}\cdot\boldsymbol{p}/|\boldsymbol{s}\cdot\boldsymbol{p}|$.
[12] J. Kirschner, *Polarized Electrons at Surfaces*, Springer, Heidelberg, **1985**; F. Meier, D. Pescia, *Phys. Rev. Lett.* **1981**, *47*, 374–377; F. Meier, G. L. Bona, S. Hufner, *Phys. Rev. Lett.* **1984**, *52*, 1152–1155; G. Borstel, M. Wohlecke, *Phys. Rev. B* **1982**, *26*, 1148–1155.
[13] R. Naaman, A. Haran, A. Nitzan, D. Evans, M. Galperin, *J. Phys. Chem. B* **1998**, *102*, 3658–3668.
[14] K. Ray, S. P. Ananthavel, D. H. Waldeck, R. Naaman, *Science* **1999**, *283*, 814–816.
[15] The asymmetry parameter is defined as $A \equiv (I_{+P} - I_{-P})/(I_{+P} + I_{-P})$ where I_{+P} and I_{-P} are the transmission of the electron beam with spin angular momentum oriented parallel (+) and antiparallel (−) to its velocity vector.
[16] W. G. J. Hol, P. T. van Duijnen, H. J. C. Berendsen, *Nature* **1978**, *273*, 443–446.
[17] C. Park, W. A. Goddard III, *J. Phys. Chem. B* **2000**, *104*, 7784–7789.
[18] Z. Vager, R. Naaman, *Chem. Phys.*, in press.
[19] The change in the work function $\Delta e\Phi$ is related to the dipole of the layer by the equation $\Delta e\Phi = 4\pi D$, where D is the dipole density. We assumed that the layer density is 5×10^{14} molecules cm^{-2}.
[20] D. M. Taylor, G. F. Bayes, *Phys. Rev. E* **1994**, *49*, 1439–1449.
[21] C.-X. Wu, M. Iwamoto, *Phys. Rev. B* **1997**, *55*, 10922–10930.
[22] E. Vélu, C. Dupas, D. Renard, J. P. Renard, J. Seiden, *Phys. Rev. B* **1988**, *37*, 668–671.
[23] A. Filipe, H.-J. Drouhin, G. Lampel, Y. Lassailly, J. Nagle, J. Peretti, V. I. Safarov, A. Schuhl, *Phys. Rev. Lett.* **1998**, *80*, 2425–2428.
[24] R. von Helmolt, J. Wecker, B. Holzapfel, L. Schultz, K. Samwer, *Phys. Rev. Lett.* **1993**, *71*, 2331–2333.
[25] S. Jin, T. H. McCormack, R. A. Dastnacht, R. Ramesh, L. H. Chen, *Science* **1994**, *264*, 413–415.

A Nanoporous Metal–Organic Framework Based on Bulky Phosphane Ligands**

Xingling Xu, Mark Nieuwenhuyzen, and Stuart L. James*

Metal–organic frameworks are polymer networks consisting of metal ions connected by organic bridging ligands, and they represent a new approach to the synthesis of nanoporous materials.[1–11] Applications are therefore anticipated as novel molecular sieves, sensors, ion-exchangers, and catalysts.[1–10] However, mutual interpenetration of the polymer networks, whereby the vertices of one occupy the cavities of another,[8, 12] often frustrates attempts to generate large accessible pores. Whereas all previous work in this field has featured N- or O- donor bridging ligands, we report novel results with a bulky triphosphane 1,3,5-tris(diphenylphosphanyl)benzene (**L**; see Figure 1a).[13, 14] The use of the ligand **L** unexpectedly gave a non-interpenetrating network polymer $[Ag_4\mathbf{L}_3(O_3SCF_3)_4]$ (**1**) with remarkably wide (1.60–1.84 nm) channels. In the as-synthesized state these channels appear to be saturated with solvent, which can be exchanged for other solvents, which can be removed by heating under vacuum without collapse of the metal–phosphane framework. The network bulk, imparted by the phenyl groups of **L**, seems to disallow network interpenetration. Because a P-donor ligand was used, ^{31}P NMR spectroscopy gives insight into solution-state precursors, which appear to be discrete coordination cages.

We have investigated the coordination-cage and polymer chemistry of multidentate phosphane silver complexes.[15a–d] For example, the flexible triphosphane $CH_3C(CH_2PPh_2)_3$ (triphos) unexpectedly gave the hexasilver adamantanoid cage $[Ag_6(triphos)_4(triflate)_4]^{2+}$ (triflate = trifluoromethanesulfonyl).[15a] Given the differences in behavior of flexible[16] and rigid[15b,c] diphosphanes, we were interested in how the rigid triphosphane **L** would behave. Polymer **1** was obtained by diffusing diethyl ether into a chloroform–nitromethane solution containing a 3:2 molar ratio of silver trifluoromethanesulfonate (silver triflate, AgOTf) and **L**. Polymer **1** was initially isolated as hexagonal crystals in 10% yield, the remainder of the product being a powder which X-ray diffraction showed to be amorphous.[17] A single-crystal X-ray analysis of **1**,[18] performed on a crystal which was mounted rapidly after removal from the supernatant, and cooled to 120 K, revealed a two-dimensional network of hexagonal rings (Figure 1b). The large 72-atom rings contain 18 silver atoms and 12 **L** units. The network nodes are trigonal-planar silver centers bonded to three **L** units, with neighboring triflate anions which are too distant for significant bonding interactions (Ag···O distance 3.25(1) Å). The connectors between the nodes are $Ag_2\mathbf{L}_2$ groups which have a 12-membered ring structure. The pairs of silver centers in these smaller rings each bond to two P atoms and are bridged by two weakly coordinated triflate anions, each making two Ag···O contacts of 2.73(1) and 2.93(1) Å. The CF_3 groups of these triflate anions point towards the centers of the large rings, to give a transannular F···F distance of 19.01(3) Å, which corresponds to approximately 16.0 Å when the van der Waals radius of fluorine (1.47 Å[19]) is taken into account. The transannular H···H distance between phenyl groups is 20.8 Å, which gives a major ring diameter of around 18.4 Å when the H van der Waals radius of 1.20 Å[19] is taken into account. The honeycomb layers stack in an eclipsed fashion, so that a three-dimensional structure of approximately cylindrical channels is generated. A space-filling representation of a segment of the framework (nine channels and five layers), which includes the phenyl groups, is shown in Figure 1c. These channels are amongst the widest reported so far for a coordination network. In fact, the calculated "free sphere" (i.e. the largest sphere which could move freely throughout the structure, a parameter introduced by Yaghi and co-workers[20]) of diameter 16.0 Å may be the largest of any characterized crystal. Of note is the superficial similarity of **1** to the liquid crystal templated SiO_2-framework MCM-41s,[21, 22] which have channel diameters of around 15 to 100 Å, but are not ordered at the atomic level. Based on a spherical

[*] Dr. S. L. James, Dr. X. Xu, Dr. M. Nieuwenhuyzen
School of Chemistry
The Queen's University of Belfast
David Keir Building, Stranmillis Road, Belfast, Northern Ireland BT9 5AG (UK)
Fax: (+44) 28 90 38 21 17
E-mail: s.james@qub.ac.uk

[**] We thank the McClay Trust and the EPSRC for funding, and are grateful to the referees for their suggestions.

  1433-7851/02/4105-0764 $ 17.50+.50/0